

UDC 537.6; 538.9; 548.3

**CRYSTAL STRUCTURE AND MAGNETIC PROPERTIES
OF $(\text{Cr}_{0.34}\text{Cu}_{0.10}\text{Ni}_{0.56})_4\text{Si}$**

**R.-I. Martyniak^{1*}, N. Muts¹, A. Horyn¹, Ya. Tokaychuk¹, M. Bobnar²,
L. Akselrud^{1,3}, R. Gladyshevskii¹**

¹*Department of Inorganic Chemistry, Ivan Franko National University of Lviv,
Kyryla i Mefodiya Str., 6, 79005 Lviv, Ukraine;*

²*Department of Condensed Matter Physics, Jožef Stefan Institute,
Jamova Cesta, 39, 1000 Ljubljana, Slovenia;*

³*Max Planck Institut für Chemische Physik fester Stoffe,
Nöthnitzer Straße, 40, 01187 Dresden, Germany
e-mail: martyniak241@gmail.com*

The crystal structure of the π phase $(\text{Cr,Cu,Ni})_4\text{Si}$ was refined from X-ray powder diffraction data and found to belong to the βMn structure family, namely, to the structure type Au_4Al (Pearson symbol $cP20$, space group $P2_13$): unit-cell parameter $a = 0.612269(8)$ nm for $(\text{Cr}_{0.34(1)}\text{Cu}_{0.10(1)}\text{Ni}_{0.56(1)})_4\text{Si}$ (composition from EDS). The temperature dependence of the magnetic susceptibility of a sample of nominal composition $\text{Cr}_{26}\text{Cu}_9\text{Ni}_{47}\text{Si}_{18}$, containing more than 96 wt.% of the title compound, revealed Curie-Weiss paramagnetism: $\chi_0 = 1.42 \cdot 10^{-4}$ emu g-at⁻¹, $C = 2.7 \cdot 10^{-3}$ emu g-at⁻¹ K⁻¹, $\theta_p = -41$ K. Cu doping decreased the paramagnetic temperature to more negative values.

Keywords: X-ray powder diffraction, crystal structure, magnetic properties, magnetic skyrmions.

DOI: <https://doi.org/10.30970/vch.6101.093>

1. Introduction

Globalization trends in the modern world create a need for efficient and reliable data storage technology. Current data storage devices have significant flaws, *e.g.* they have too low information storage density and are sensitive to external conditions. These problems can, however, be addressed by using novel quantum materials. Skyrmionic materials, ferromagnets containing whirling nanoscopic spin texture defects called magnetic skyrmions, may one day supersede the classical ferromagnetic materials used in RAM (Random Access Memory) and DWM (Domain Wall Memory) technologies [1]. Their superiority over the usual ferromagnets lies in the small size of a magnetic skyrmion (sometimes less than 10 nm) and the simplicity of skyrmion manipulation in a conductor. These two factors justify the interest in industrial synthesis of skyrmionic materials.

The aforementioned merits of skyrmionic materials have directed our research into this area. The existence of magnetic skyrmions in a conductor is restricted by two conditions: one structural and the other one magnetic. On the one hand, magnetic skyrmions

can only be nucleated in solids crystallizing in one of the 22 enantiomorphic space groups. On the other hand, a skyrmionic spin state is only observed for materials having a slightly positive paramagnetic Curie temperature. This work is a continuation of previous investigations [2–5] on the π phase in the Cr–Ni–Si system [6] and the effect of element substitution on the crystal structure and magnetic properties, and presents the results of investigations of a $\text{Cr}_{26}\text{Cu}_9\text{Ni}_{47}\text{Si}_{18}$ alloy.

2. Materials and experimental procedures

A sample of nominal composition $\text{Cr}_{26}\text{Cu}_9\text{Ni}_{47}\text{Si}_{18}$ was prepared by arc-melting of pure (≥ 99.9 wt. %) elements under a purified argon atmosphere. The mass of the alloy was 1 g and the loss during the preparation was less than 1 % of the total mass. The alloy was annealed at 1173 K for 35 days in an evacuated quartz ampoule, and quenched in cold water thereafter. The crystal structure was refined from X-ray powder diffraction data recorded with a Huber Image Plate Camera G670 diffractometer (Cu $K\alpha_1$ radiation), using the FullProf Suite package [7]. The temperature dependence of the magnetic susceptibility was measured on a SQUID magnetometer (MPMS-XL7, Quantum Design) in external fields of 3.5 and 7.0 T in the temperature range 1.8–300 K. A high-temperature differential scanning calorimetry (DSC) curve of the $\text{Cr}_{26}\text{Cu}_9\text{Ni}_{47}\text{Si}_{18}$ alloy was obtained using a Linseis simultaneous thermo analytical instrument STA PT 1600 in a dynamic atmosphere of argon (~ 6 dm³/h) with heating/cooling rates of 10 K/min in the temperature range between 293 and 1423 K.

The elemental composition of the sample was determined using energy-dispersive X-ray spectroscopy (EDS) using an X-Max^N microanalysis system and a scanning electron microscope (SEM) Tescan Vega 3. The compositions of the individual phases present in the sample were determined by EDS analysis using AZtecLive real-time chemical imaging powered by an X-Max^N Silicon Drift Detector.

3. Results and discussion

The result of the EDS analysis of the $\text{Cr}_{26}\text{Cu}_9\text{Ni}_{47}\text{Si}_{18}$ sample showed good agreement with the nominal composition (Table 1). The sample was found to contain two phases: a main phase (gray region) with the composition $\text{Cr}_{28.1(6)}\text{Cu}_{4.7(6)}\text{Ni}_{48(1)}\text{Si}_{19.2(6)}$ and a secondary phase (pale gray regions) with the composition $\text{Cu}_{76(5)}\text{Ni}_{17(3)}\text{Cr}_{6(2)}\text{Si}_{1.0(5)}$ (Fig. 1).

A complete structure refinement using the Rietveld method was performed on X-ray powder diffraction data obtained for the $\text{Cr}_{26}\text{Cu}_9\text{Ni}_{47}\text{Si}_{18}$ sample (Fig. 2). The phase analysis showed that the alloy contained, as expected, as main component the (Cr, Cu, Ni)₄Si phase crystallizing in the enantiomorphic space group $P2_13$ (structure type Au_4Al , which is an ordered derivative of the βMn type, Pearson symbol $cP20$ [8]). However, the sample was also found to contain approximately 4 wt.% of an additional phase based on elementary Cu dissolving mainly Ni (structure type Cu, Pearson symbol $cF4$, space group $Fm-3m$ [8]). The positional coordinates and isotropic displacement parameters of the atoms in the structure of $(\text{Cr}_{0.34(1)}\text{Cu}_{0.10(1)}\text{Ni}_{0.56(1)})_4\text{Si}$ are given in Table 2; details of the structural refinement are summarized in Table 3. The cell parameter of the title compound, 0.612269(8) nm, is very close to the value reported for the π phase in the Cr–Ni–Si system (0.6120 nm [8]). Due to the similar number of electrons of the constituting metal atoms, the statistical mixture of Cr, Ni, and Cu atoms at the Wyckoff positions $12b$ and $4a$ in the (Cr, Cu, Ni)₄Si phase was fixed at $M1 = M2 = \text{Cr}_{0.34}\text{Cu}_{0.10}\text{Ni}_{0.56}$, *i.e.* the proportions determined by the EDS analysis. The cell parameter of the (Cu, Ni) solid solution containing small amounts of Cr and Si, 0.360171(7) nm, is also in good agreement with values for (Cu, Ni) reported in the literature [8].

Table 1

Results (at.%) of the EDS investigation of the $\text{Cr}_{26}\text{Cu}_9\text{Ni}_{47}\text{Si}_{18}$ sample

Element	Overall composition	Main phase	Secondary phase
Cr	27.4	28.1(6)	6(2)
Cu	8.4	4.7(6)	76(5)
Ni	45.8	48(1)	17(3)
Si	18.4	19.2(6)	1.0(5)

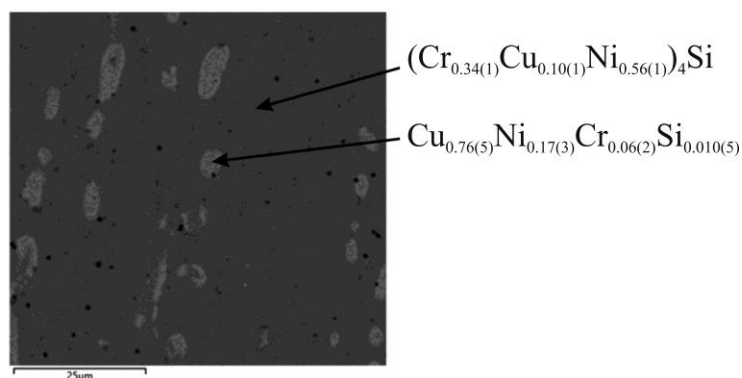


Fig. 1. SEM photograph of the $\text{Cr}_{26}\text{Cu}_9\text{Ni}_{47}\text{Si}_{18}$ sample:
 gray matrix – $(\text{Cr}_{0.34(1)}\text{Cu}_{0.10(1)}\text{Ni}_{0.56(1)})_4\text{Si}$; light gray regions – $\text{Cu}_{0.76(5)}\text{Ni}_{0.17(3)}\text{Cr}_{0.06(2)}\text{Si}_{0.010(5)}$

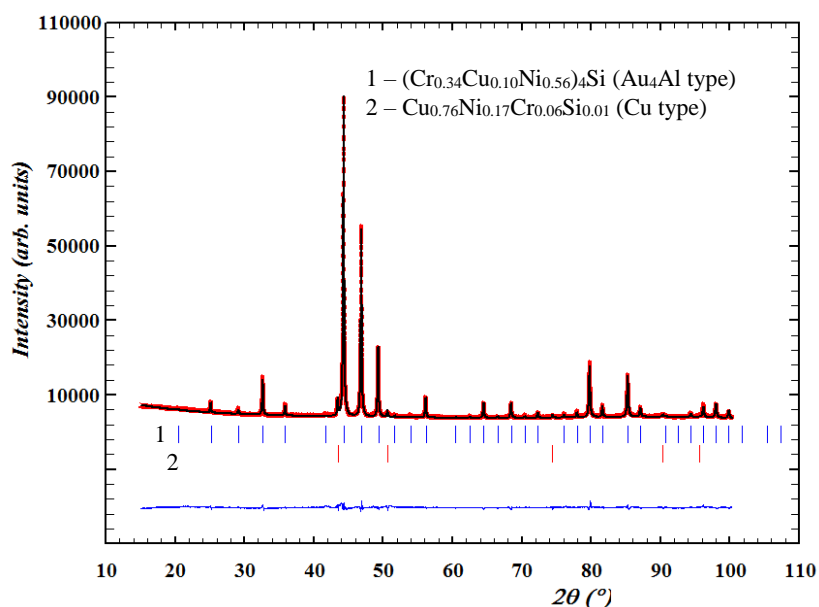


Fig. 2. Observed, calculated and difference (bottom) X-ray powder diffraction patterns for the $\text{Cr}_{26}\text{Cu}_9\text{Ni}_{47}\text{Si}_{18}$ sample annealed at 1173 K for 35 days; Cu $K\alpha_1$ radiation ($\lambda = 0.154060$ nm)

Table 2

Atomic coordinates and isotropic displacement parameters for $(\text{Cr}_{0.34}\text{Cu}_{0.10}\text{Ni}_{0.56})_4\text{Si}$
(structure type Au_4Al , Pearson symbol $cP20$, space group $P2_13$)

Site	Wyckoff position	Atomic coordinates			B_{iso} (10^2 nm^2)
		x	y	z	
$M1$	$12b$	0.79689(15)	0.95313(13)	0.37842(19)	1.42(2)
$M2$	$4a$	0.68571(16)	0.68571(16)	0.68571(16)	1.36(5)
Si	$4a$	0.0695(3)	0.0695(3)	0.0695(3)	0.49(7)

 $M1 = M2 = \text{Cr}_{0.34}\text{Cu}_{0.10}\text{Ni}_{0.56}$.

Table 3

Experimental details and crystallographic data for the individual phases in the $\text{Cr}_{26}\text{Cu}_9\text{Ni}_{47}\text{Si}_{18}$ alloy

Phase	$(\text{Cr}_{0.34}\text{Cu}_{0.10}\text{Ni}_{0.56(1)})_4\text{Si}$	$\text{Cu}_{0.76}\text{Ni}_{0.17}\text{Cr}_{0.06}\text{Si}_{0.01}$
Content, wt. %	96.3(3)	3.7(3)
Structure type	Au_4Al	Cu
Pearson symbol	$cP20$	$cF4$
Space group	$P2_13$	$Fm\bar{3}m$
Unit cell parameter a , nm	0.612269(8)	0.360171(7)
Cell volume, nm^3	0.229523(5)	0.046722(2)
Density D_x , g cm^{-3}	8.222	8.896
Diffractometer	Huber Image Plate Camera – G670	
Radiation λ , nm	Cu $K\alpha$, 0.154060	
Scanning mode	$\theta/2\theta$	
Range of 2θ , $^\circ$	15.00–110.35	
Step size, $^\circ$	0.005	
Profile parameters U, V, W	0.037(3), –0.014(3), 0.023(9)	
Asymmetry parameters	–0.001(2), –0.0006(4)	
Reliability factors R_B	7.46	18.7
R_F	9.58	9.93
R_p, R_{wp}, χ^2	2.20, 3.02, 4.55	

The $\text{Cr}_{26}\text{Cu}_9\text{Ni}_{47}\text{Si}_{18}$ sample was also investigated by high-temperature differential scanning calorimetry. In an earlier investigation of the Cr–Ni–Si system [9] the π phase was observed at 1123 K, but not at 1073 K, which seemed to indicate a eutectoid decomposition taking place between these two temperatures. The DSC curve of the $\text{Cr}_{26}\text{Cu}_9\text{Ni}_{47}\text{Si}_{18}$ sample (Fig. 3) exhibits two peaks. The first, narrow peak appears at 1293–1297 K, and the second, broader, asymmetric peak at 1347–1373 K. Such a diagram may describe incongruent melting of the main phase, where the former peak corresponds to the solidus (melting temperature) and the latter to the liquidus. Five different ternary phases were observed in the isothermal section of the phase diagram of the Cr–Ni–Si system at 1123 K [9], some of them in a relatively narrow composition region, increasing the probability of incongruent melting. Melting of the additional phase identified as a solid solution based on (Cu, Ni) with low amounts of Cr and Si (composition from EDS analysis $\text{Cr}_{6(2)}\text{Cu}_{76(5)}\text{Ni}_{17(3)}\text{Si}_{1.0(5)}$) is expected to occur close to the experimental limit of the investigation (1423 K). Elementary Cu forms a continuous solid solution with Ni, where the melting point steadily increases from 1358 K for Cu to 1728 K for Ni [10] and 17 at. % Ni corresponds to approximately 1423 K. Pure Cu dissolves less than 1 at. % Cr, but Ni dissolves up to 50 at. % Cr, which reduces the melting point to 1618 K. From our investigations, including earlier DSC of a $\text{Cr}_{30}\text{Ni}_{50}\text{Si}_{20}$ sample [2], we see no indication of a eutectoid decomposition or other transition of the π phase in the temperature range between 1073 and 1123 K.

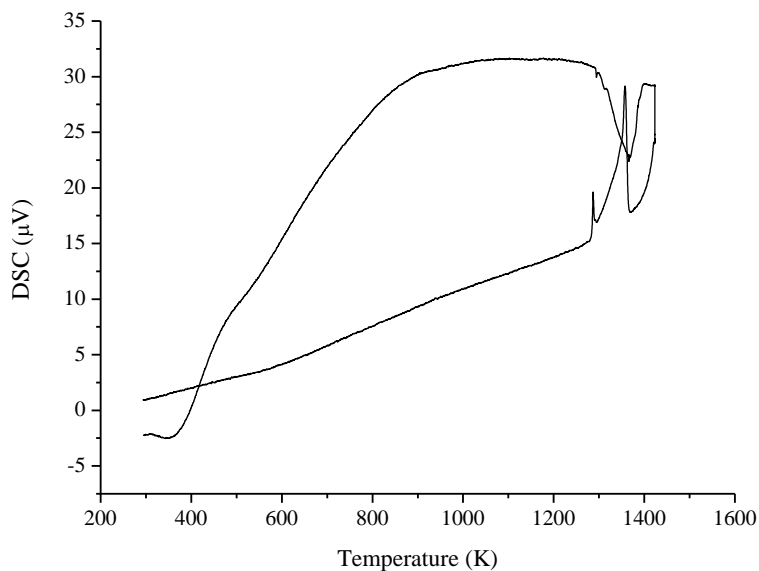


Fig. 3. DSC curve for the $\text{Cr}_{26}\text{Cu}_9\text{Ni}_{47}\text{Si}_{18}$ sample

The parent $(\text{Cr}, \text{Ni})_4\text{Si}$ phase shows Curie-Weiss paramagnetic behavior with a paramagnetic Curie temperature from -13 K to -15 K [3]. Magnetic measurements of the $\text{Cr}_{26}\text{Cu}_9\text{Ni}_{47}\text{Si}_{18}$ sample were performed in two magnetic fields (3.5 and 7.0 T). The temperature dependence of the magnetic susceptibility in the range 1.8–300 K, shown in Fig. 4, revealed paramagnetic behavior above 20 K also for the Cu-doped sample.

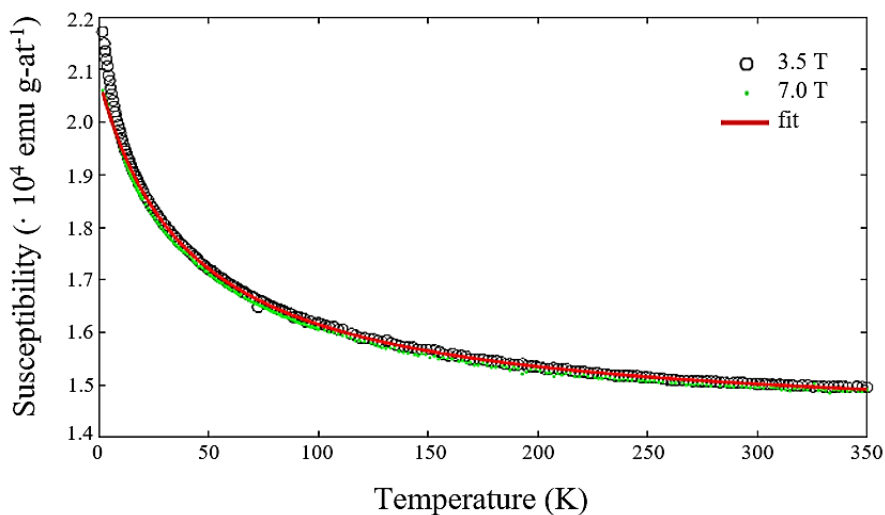


Fig. 4. Temperature dependence of the magnetic susceptibility of the $\text{Cr}_{26}\text{Cu}_9\text{Ni}_{47}\text{Si}_{18}$ alloy, measured in magnetic fields of 3.5 and 7.0 T. The red solid line shows the modified Curie-Weiss fit at 3.5 T

The use of two different fields showed that the susceptibility is slightly field-dependent, which can be attributed to a tiny ferromagnetic impurity, equivalent to 5 ppm of metallic iron. It is known that elementary Ni is a ferromagnet, and the solid solution (Cu, Ni) remains ferromagnetic with T_C decreasing with increasing Cu content. The data obtained at 3.5 T were fit to a modified Curie-Weiss law $\chi = \chi_0 + C/(T-\theta_p)$, where $C = 2.7 \cdot 10^{-3}$ emu g-at⁻¹ K⁻¹ is the Curie constant, $\theta_p = -41$ K is the paramagnetic Curie temperature, and $\chi_0 = 1.42 \cdot 10^{-4}$ emu g-at⁻¹ is the temperature-independent contribution to the susceptibility. The negative Curie temperature indicates antiferromagnetic interactions and the effective magnetic moment μ_{eff} calculated from the Curie constant is $0.147 \mu_B/\text{atom}$. χ_0 is the sum of a positive Pauli paramagnetic contribution of the conduction electrons χ_{Pauli} and a negative diamagnetic contribution of the core electrons $\chi_{\text{dia}} = -7.59 \cdot 10^{-6}$ emu g-at⁻¹, which was calculated for Cr⁶⁺, Cu²⁺, Ni²⁺, and Si⁴⁺ ions [11]. Thus, the contribution of the conduction electrons equals $\chi_{\text{Pauli}} = \chi_0 - \chi_{\text{dia}} = 1.49 \cdot 10^{-4}$ emu g-at⁻¹, which corresponds to a density of states at the Fermi level $g(E_F) = 4.61$ states/(eV atom). This is higher than the density of states at the Fermi level of metallic Ni (4.06 states/(eV atom)) and indicates electron correlations and an enhancement of the susceptibility. A phase with Au₄Al-type structure is also known in the Fe–Ni–Si system [12] with a relatively broad homogeneity range extending along the isoconcentrate 20 at. % Si. This phase exhibits ferromagnetic order with a Curie temperature of 550–650 K, depending on the Fe content, for the same structure type. Our previous attempts to partially replace Cr and/or Ni by Fe, Ru, Co, or Pd in the (Cr, Ni)₄Si phase, revealed the following paramagnetic Curie temperatures for samples of nominal composition Cr₂₈M₅Ni₄₉Si₁₈: -7 K for M = Fe [4], Cr₂₇M₅Ni₄₈Si₂₀: -52 K for M = Co [3], *i.e.* in all these cases the interactions remained antiferromagnetic.

4. Conclusions

The crystal structure of the Cu-doped π phase (Cr, Ni)₄Si was refined from X-ray powder diffraction data of a Cr₂₆Cu₉Ni₄₇Si₁₈ sample annealed at 1173 K. Most of the Cu had been incorporated, but the alloy contained two phases: the quantitatively predominant (96.3(3) wt. %) (Cr_{0.34(1)}Cu_{0.10(1)}Ni_{0.56(1)})₄Si phase and a (Cu, Ni)-based solid solution of composition Cu_{0.76(5)}Ni_{0.17(3)}Cr_{0.06(2)}Si_{0.010(5)} (3.7 wt. %). Measurements of the temperature dependence of the magnetic susceptibility showed paramagnetic behavior. As previously observed for doping by Co ($\theta_p = -52$ K) [3], substitution of Cu atoms for Cr and Ni led to a significant decrease of the value of the paramagnetic Curie temperature ($\theta_p = -41$ K), compared to values between -13 and -15 K for the parent phase. Previous substitution by Fe, Ru, or Pd reduced the absolute value of θ_p , but the interactions remained antiferromagnetic [4, 5].

The enantiomorphic crystal structure of the title compound was confirmed, however, magnetic properties propitious for the formation of skyrmions, *i.e.* a slightly positive paramagnetic Curie temperature, were not obtained by replacing Cr and/or Ni by Cu.

Acknowledgements

We thank Dr Karin Cenzual from Geneva University for useful discussions.

1. *Fert A., Reyren N., Cros V.* Magnetic Skyrmions: Advances in Physics and Potential Applications // *Nat. Rev. Mater.* 2017. Vol. 2. P. 17031.
DOI: <http://dx.doi.org/10.1038/natrevmats.2017.31>
2. *Martyniak R.-I., Muts N., Akselrud L., Gladyshevskii R.* Synthesis and Structural Investigation of Samples in the Cr–Ni–Si System // *Visn. Lviv Univ. Ser. Khim.* 2018. Vol. 59. P. 76–82 (in Ukrainian). DOI: <http://dx.doi.org/10.30970/vch.5901.076>
3. *Martyniak R.-I., Muts N., Sichevych O., Borrmann H., Bobnar M., Akselrud L., Gladyshevskii R.* Structure and Magnetic Properties of (Cr, Ni)_{4-x}Co_xSi // *Solid State Phenom.* 2019. Vol. 289. P. 108–113.
DOI: <http://dx.doi.org/10.4028/www.scientific.net/SSP.289.108>
4. *Martyniak R.-I., Muts N., Bobnar M., Akselrud L., Gladyshevskii R.* Structure and Magnetic Properties of (Cr, T, Ni)₄Si Phases (T = Cu, Fe, Pd) // *Book Abstr. Int. Conf. Stud. Young Scient. Theor. Exper. Phys. "HEUREKA-2019"*. 2019. Lviv. P. A14.
5. *Martyniak R.-I., Muts N., Bobnar M., Akselrud L., Gladyshevskii R.* Crystal Structure and Magnetic Properties of Cr–{Ru, Pd}–Ni–Si Phases // *Coll. Abstr. XIV Int. Conf. Cryst. Chem. Intermet. Compd.* 2019. Lviv. P. 150.
6. *Gladyshevskii E. I., Kripyakevich P. I., Kuz'ma Yu. B.* The Crystal Structure of Low-Silicon Ternary Compounds in the Cr–Ni–Si and Cr–Co–Si Systems // *J. Struct. Chem.* 1962. Vol. 3. P. 402–410.
7. *Rodriguez-Carvajal J.* Recent Developments of the Program FullProf // *Newsletter in Commission on Powder Diffraction (IUCr)*. 2001. Vol. 26. P. 12–19.
8. *Villars P., Cenzual K.* (Eds.) *Pearson's Crystal Data – Crystal Structure Database for Inorganic Compounds*, ASM International: Materials Park, OH, USA, Release 2017/18.
9. *Gladyshevskii E. I., Borusevich L. K.* The Cr–Ni–Si Ternary System // *Russ. J. Inorg. Chem.* 1963. Vol. 8. P. 997–1000.
10. *Chakrabarti D. J., Laughlin D. E., Shen S. W., Chang Y. A.* Cu–Ni (Copper-Nickel) Binary Alloy Phase Diagrams // *T. B. Massalski (Ed.), ASM International: Materials Park, OH, USA.* 1990. Vol. 2. P. 1442–1446.
11. *Selwood P. W.* *Magnetochemistry*, 2nd Ed. // Interscience. New York, USA, 1956.
12. *Ackerbauer S., Krendelsberger N., Weitzner F., Hiebl K., Schuster J. C.* The Constitution of the Ternary System Fe–Ni–Si // *Intermetallics*. 2009. Vol. 17. P. 414–420.

**КРИСТАЛІЧНА СТРУКТУРА ТА МАГНІТНІ ВЛАСТИВОСТІ
(Cr_{0,34}Cu_{0,10}Ni_{0,56})₄Si****Р.-І. Мартиняк^{1*}, Н. Муць¹, А. Горинь¹, Я. Токайчук¹, М. Бобнар²,
Л. Аксельруд^{1,3}, Р. Гладішевський¹**

¹*Кафедра неорганічної хімії,
Львівський національний університет імені Івана Франка,
вул. Кирила і Мефодія, 6, 79005 Львів, Україна;*

²*Кафедра фізики конденсованих систем, Інститут Йозефа Стефана,
вул. Ямова, 39, 1000 Любляна, Словенія;*

³*Інститут хімічної фізики твердого тіла Товариства Макса Планка,
вул. Нотніцер, 40, 01187 Дрезден, Німеччина
e-mail: martyniak241@gmail.com*

Описано спробу одержання скірміонного матеріалу. Магнітні скірміони – наноскопічні вихроподібні дефекти спінової текстури феромагнетиків, які завдяки своєму компактному розміру становлять науковий та індустріальний інтерес щодо їхнього застосування у пристроях збереження та відтворення інформації. Використання скірміонних матеріалів у пристроях цього типу може суттєво збільшити густину запису даних, що є надзвичайно актуальним у XXI ст. Існування магнітних скірміонів у кристалах обмежується структурною та магнітною умовами, які полягають у тому, що структура скірміонного матеріалу повинна бути нецентросиметричною, а парамагнітна температура Кюрі – додатною.

Проведено повне уточнення кристалічної структури фаз полікристалічного зразка Cr₂₆Cu₉Ni₄₇Si₁₈ методом Рітвельда на основі дифракційних даних. З'ясовано, що в цьому зразку кількісно переважає фаза складу (Cr_{0,34(1)}Cu_{0,10(1)}Ni_{0,56(1)})₄Si (96.3(3) мас. %). Кристалічна структура цієї фази належить до структурного типу Au₄Al (символ Пірсона cP20, просторова група P2₁3); параметр елементарної комірки $a = 0,612269(8)$ нм для (Cr_{0,34(1)}Cu_{0,10(1)}Ni_{0,56(1)})₄Si (склад визначено енергодисперсійною рентгенівською спектроскопією). Тип Au₄Al належить до родини структур, похідних до βMn.

Зразок Cr₂₆Cu₉Ni₄₇Si₁₈ досліджували методом високотемпературної диференціальної скануючої калориметрії. Аналіз отриманої кривої засвідчив відсутність будь-яких перетворень для фази (Cr_{0,34(1)}Cu_{0,10(1)}Ni_{0,56(1)})₄Si в температурному інтервалі 293–1123 К.

Для зразка Cr₂₆Cu₉Ni₄₇Si₁₈ досліджено температурну залежність магнітної сприйнятливості у магнітних полях індукцією 3,5 та 7,0 Тл. Уточнено, що для сполуки властивий Кюрі-Вайсовський парамагнітний характер магнітного впорядкування: $\chi_0 = 1,42 \cdot 10^{-4}$ е.м.о. г·ат⁻¹; $C = 2,7 \cdot 10^{-3}$ е.м.о. г·ат⁻¹ К⁻¹; $\theta_P = -41$ К у магнітному полі індукцією 3,5 Тл.

Ключові слова: рентгенівська порошкова дифракція, кристалічна структура, магнітні властивості, магнітні скірміони.

Стаття надійшла до редколегії 04.11.2019
Прийнята до друку 19.02.2020